Int. J. Heat Mass Transfer. Vol. 34, No. 12, pp. 3107–3120, 1991
Printed in Great Britain

0017–9310/91 $3.00 + 0.00

Natural convection due to horizontal temperature and concentration gradients—1. Variable thermophysical property effects

J. A. WEAVER and R. VISKANTA
Heat Transfer Laboratory, School of Mechanical Engineering, Purdue University, West Lafayette, IN 47907, U.S.A.

(*Received* 26 *January* 1990 *and in final form* 10 *December* 1990)

Abstract—Typically for single component fluids, the variation of thermophysical properties is negligible except in the presence of large temperature differences, and, therefore, has no appreciable effect on the heat transfer. In contradistinction, thermophysical properties can vary significantly due to concentration differences which affect the heat and mass transfer. This work examines the effects of thermophysical property variation on the heat and mass transfer in a cavity due to natural convection driven by combined thermal and solutal buoyancy forces. Results indicate that thermophysical property variations can appreciably influence heat and mass transfer and velocity distribution.

INTRODUCTION

FEW SYSTEMS in nature exist as a pure, single component, but more importantly, advanced technological and industrial processes involve multicomponent fluids. Some of the applications include building technology, crystal growth by physical or chemical vapor deposition, vapor deposition of thin films, drying processes and geophysical problems. The range of Grashof number varies significantly among these applications (e.g. $Gr \approx 1 \times 10^2$–1×10^4 for crystal growth and $1 \times 10^{12} < Gr < 1 \times 10^{14}$ for certain geophysical applications). Much of the work in the past has been concerned with natural convection in single component fluids, and some current reviews are available [1–5]. More specifically, Ostrach [6] has reviewed natural convection work due to combined driving forces and indicates inadequacies and areas where further research would be beneficial. A greater portion of the review of existing work dealt with free convection from vertical surfaces. Discussion of internal flows in enclosures concerned fluids with a large Prandtl number (liquids) and no mention was made of studies with gases as the working fluid. Because crystal growth from the vapor is a major application of natural convection in binary gases, some reviews have been reported [7–12]. These articles point out the difficulties in obtaining both analytical and experimental results of the complex process of natural convection due to combined driving forces. Furthermore, it is made clear that there are large gaps in the existing knowledge. The more pertinent, recent literature concerning natural convection of binary gases in enclosures is reviewed below.

Rosenberger and co-workers [13–16] numerically simulated diffusive physical vapor transport in two dimensions. Furthermore, the possibility of different orientations of the enclosure with respect to the gravity vector was examined. The Schmidt and Prandtl numbers were shown to have a significant influence on the transport of the crystal component. Some assumptions were made which limit the scope of the results. More recently, Ranganathan and Viskanta [17] have performed an analytical–numerical study examining natural convection with constant thermophysical properties due to combined driving forces which presents numerical results from a parametric study.

Trevisan and Bejan [18] considered flow in a cavity which lies in the boundary layer regime. An Oseen-linearized solution is reported for $Le = 1.0$. A similarity solution is also described which removes the restriction of $Le = 1.0$ from the analysis. Confidence in the analytical solution is gained by numerically solving the equations using the control volume approach of Patankar [19]. Consideration of the boundary layer regime limits the scope of the analytical results. Lai and Ramsey [20] investigated specifically the transport of water vapor and air in a cavity. A combined Grashof number (weighted sum of solutal and thermal Grashof numbers) was used to show the influence of the thermal and solutal gradients on the flow structure in the cavity and Nusselt number. Furthermore, Wee *et al.* [21] investigated the heat and moisture transfer by natural convection in a rectangular cavity with regards to the application of heat and mass transfer in building cavities. Some experiments were performed to measure the average Sherwood and Nusselt numbers which agreed well with numerical predictions.

As recently as 1980, in a critical review of natural convection with combined driving forces Ostrach [6] cites no work performed with binary gases in a cavity. Earlier numerical work which addressed this problem made assumptions such as the species and/or temperature distribution, the solutal buoyancy effect or species interdiffusion, Soret and Dufour effects were negligible. Therefore, the actual problem solved only

NOMENCLATURE

A_z	L/H
c_p	specific heat at constant pressure of binary mixture
c_p^*	specific heat ratio, c_p/c_{pr}
C_T	$T_C/(T_H-T_C)$
C_{wv}	$(1-\omega_C)/(\omega_H-\omega_C)$
D_{AB}	binary mass diffusion coefficient
D_{AB}^*	binary mass diffusion coefficient ratio, D_{AB}/D_{ABr}
Gr	Grashof number, $g\beta_T(T_H-T_C)H^3/\nu_r^2$
h	enthalpy or heat transfer convection coefficient
h_m	mass transfer convection coefficient
H	test cavity height
k	thermal conductivity of binary mixture
k^*	thermal conductivity ratio, k/k_r
L	test cavity length
Le	Lewis number, α_r/D_{ABr}
M	molecular weight
M^*	molecular weight ratio, M_A/M_B
N	buoyancy parameter, $\beta_C(\omega_H-\omega_C)/\beta_T(T_H-T_C)$
N^*	buoyancy parameter, $(\rho_C-\rho_H)/[\rho_r\beta_T(T_H-T_C)]$
Nu	Nusselt number
P	dimensionless pressure, $P_d/\rho_r U_r^2$
Pr	Prandtl number, ν_r/α_r
q	heat flux
Q	dimensionless heat flux, $qH/k_r\Delta T$
Q_a	advected energy flux
Q_d	energy flux due to diffusion
R	universal gas constant
Ra	Rayleigh number, $Gr\ Pr$
Sc	Schmidt number, ν_r/D_{ABr}
Sh	Sherwood number
T	temperature
ΔT	temperature difference across the cavity, T_H-T_C
u, w	dimensionless velocity in the ξ-direction (U/U_r) and ζ-direction (W/U_r), respectively
U_r	reference velocity, $(\nu/H)\ Gr^{0.5}$
x, z	Cartesian coordinate directed along the length and height of the test cell, respectively.

Greek symbols

α	thermal diffusivity, $k/\rho c_p$
β_C	solutal coefficient of volumetric expansion
β_T	thermal coefficient of volumetric expansion
ζ, ξ	dimensionless $z(z/H)$ and $x(x/H)$ direction, respectively
θ	dimensionless temperature, $(T-T_C)/(T_H-T_C)$
ι	dimensionless enthalpy, $(h-h_C)/(h_H-h_C)$
μ	dynamic viscosity of binary mixture
μ^*	dynamic viscosity ratio, μ/μ_r
ν	kinematic viscosity of binary mixture, μ/ρ
ρ	density of binary mixture
ρ^*	density ratio, ρ/ρ_r
ϕ	normalized mass fraction $(\omega_A-\omega_C)/(\omega_H-\omega_C)$
ω	mass fraction
ω_H, ω_C	mass fraction of species A at the hot wall and at the cold wall, respectively
$\Delta\omega_A$	concentration difference across the cavity, $\omega_H-\omega_C$.

Subscripts

A	species A
B	species B
C	cold wall
H	hot wall
r	reference value, evaluated at $(T_H+T_C)/2$ and $(\omega_H+\omega_C)/2$
w	wall
ζ	in the ζ-direction
ξ	in the ξ-direction.

revealed a part of the physics involved. Further work is required in several areas. The influence of variable thermophysical properties and the contributions of the Soret and Dufour effects and interdiffusion of species needs further detailed examination. Also, the effect of radiative heat transfer across the cavity (participating and non-participating media), different cavity orientations with respect to the gravity vector and three-dimensional effects have not been fully determined. This work addresses variable thermophysical property effects on the natural convection in binary gases with simultaneous heat and mass transfer across a cavity.

ANALYSIS

Governing equations

Consider a rectangular enclosure as shown in Fig. 1. A mass flux into the enclosure occurs at the hot end wall due to either the sublimation of a solid or evaporation of a liquid (species A). An inert carrier gas (species B) which is not soluble in species A (solid or liquid) is present in the enclosure. Condensation of species A occurs at the opposite cold end wall. In this manner, natural convection is driven by thermal and solutal gradients across the cavity. In the system described, there are no chemical reactions, heat gen-

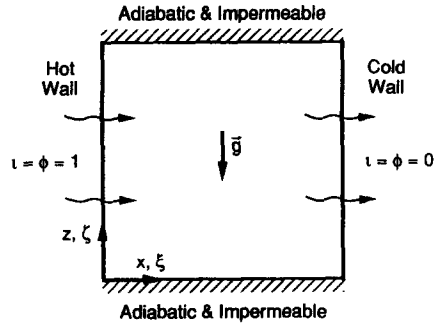

FIG. 1. Mathematical model for natural convection in binary gases with horizontal temperature and solutal gradients.

eration or heat dissipation, and the system is at steady state. The fluid motion is assumed laminar and radiative heat transfer in the cavity is neglected [22]. The resulting conservation equations of mass, momentum, energy and species, with variable properties [23] are given in dimensionless form as follows:

continuity

$$\frac{\partial}{\partial\xi}(\rho^* u)+\frac{\partial}{\partial\zeta}(\rho^* w)=0; \tag{1}$$

ξ-momentum

$$\frac{\partial}{\partial\xi}(\rho^* uu)+\frac{\partial}{\partial\zeta}(\rho^* wu)=-\frac{\partial P}{\partial\xi}+\frac{1}{\sqrt{(Gr)}}\left\{\frac{\partial}{\partial\xi}\left(\mu^*\frac{\partial u}{\partial\xi}\right)+\frac{\partial}{\partial\zeta}\left(\mu^*\frac{\partial u}{\partial\zeta}\right)+\frac{\partial}{\partial\xi}\left[\mu^*\frac{\partial u}{\partial\xi}-\tfrac{2}{3}\mu^*\left(\frac{\partial u}{\partial\xi}+\frac{\partial w}{\partial\zeta}\right)\right]+\frac{\partial}{\partial\zeta}\left(\mu^*\frac{\partial w}{\partial\xi}\right)\right\}; \tag{2}$$

ζ-momentum

$$\frac{\partial}{\partial\xi}(\rho^* uw)+\frac{\partial}{\partial\zeta}(\rho^* ww)=-\frac{\partial P}{\partial\zeta}+\frac{1}{\sqrt{(Gr)}}\left\{\frac{\partial}{\partial\xi}\left(\mu^*\frac{\partial w}{\partial\xi}\right)+\frac{\partial}{\partial\zeta}\left(\mu^*\frac{\partial w}{\partial\zeta}\right)\right\}+\left[\frac{\rho-\rho_C}{\rho_H-\rho_C}-\frac{\rho_R-\rho_C}{\rho_H-\rho_C}\right]N^*+\frac{1}{\sqrt{(Gr)}}\left\{\frac{\partial}{\partial\zeta}\left[\mu^*\frac{\partial w}{\partial\zeta}-\tfrac{2}{3}\mu^*\left(\frac{\partial u}{\partial\xi}+\frac{\partial w}{\partial\zeta}\right)\right]+\frac{\partial}{\partial\xi}\left(\mu^*\frac{\partial u}{\partial\zeta}\right)\right\}; \tag{3}$$

energy

$$\frac{\partial}{\partial\xi}(\rho^* u\iota)+\frac{\partial}{\partial\zeta}(\rho^* w\iota)=\frac{1}{Pr\sqrt{(Gr)}}\left[\frac{\partial}{\partial\xi}\left(\frac{k^*}{c_p^*}\frac{\partial\iota}{\partial\xi}\right)+\frac{\partial}{\partial\zeta}\left(\frac{k^*}{c_p^*}\frac{\partial\iota}{\partial\zeta}\right)\right]; \tag{4}$$

species A

$$\frac{\partial}{\partial\xi}(\rho^* u\phi)+\frac{\partial}{\partial\zeta}(\rho^* w\phi)=\frac{1}{Sc\sqrt{(Gr)}}\left[\frac{\partial}{\partial\xi}\left(\rho^* D_{AB}^*\frac{\partial\phi}{\partial\xi}\right)+\frac{\partial}{\partial\zeta}\left(\rho^* D_{AB}^*\frac{\partial\phi}{\partial\zeta}\right)\right]. \tag{5}$$

For ideal gases, $dh = c_p\,dT$. Taking the total derivative and rearranging yields $-k\nabla T = -(k/c_p)\nabla h$ from Fourier's law. This substitution was used in the energy equation (equation (4)) such that the equation was in terms of the enthalpy only.

The dimensionless boundary conditions on enthalpy are

$$\iota(0,\zeta)=1,\quad \iota(A_\xi,\zeta)=0 \tag{6}$$

$$\frac{\partial\iota}{\partial\zeta}=0\quad\text{at}\quad\zeta=0\quad\text{and}\quad 1. \tag{7}$$

The boundary conditions for species A are

$$\phi(0,\zeta)=1,\quad \phi(A_\xi,\zeta)=0 \tag{8}$$

$$\frac{\partial\phi}{\partial\zeta}=0\quad\text{at}\quad\zeta=0\quad\text{and}\quad 1. \tag{9}$$

The velocity boundary conditions at the impermeable walls are written in terms of dimensionless variables as

$$w(0,\zeta)=w(A_\xi,\zeta)=u(\xi,0)=w(\xi,0)=u(\xi,1)=w(\xi,1)=0. \tag{10}$$

At the endwalls where heat and mass are transported, the normal velocities are determined by a mass balance at the surface and are

$$u(0,\zeta)=\frac{1}{C_{wv}-1}\frac{1}{\rho^*\,Sc\,Gr^{1/2}}J_{A\xi}|_{\xi=0} \tag{11}$$

$$u(A_\xi,\zeta)=\frac{1}{C_{wv}}\frac{1}{\rho^*\,Sc\,Gr^{1/2}}J_{A\xi}|_{\xi=A_\xi}. \tag{12}$$

These normal velocities are not known a priori.

Dimensionless transport parameters

The Nusselt number is defined as

$$Nu=\frac{hH}{k_r}=\frac{q}{q_{cond}} \tag{13}$$

which is the total heat flux over the heat flux due to heat conduction alone across the cavity. For clarity, the dimensionless diffusive energy flux will be denoted by

$$Q_d=-k^*\frac{\partial\theta}{\partial\xi}\bigg|_{wall}. \tag{14}$$

Rewriting equation (14) in terms of the conserved property (enthalpy) yields

$$Q_d=-\frac{k^*}{c_p}\frac{h_H-h_C}{T_H-T_C}\frac{\partial\iota}{\partial\xi}\bigg|_{wall}. \tag{15}$$

When natural convection is absent, Q_d is equal to

unity. Hence, Q_d illustrates the increased heat transfer (temperature or enthalpy gradient) at the wall due to natural convection effects. With a mass flux at the surface, energy is transported at the surface by advection of fluid into or out of the cavity. Therefore, the total energy transferred at the wall includes contributions from diffusion and advection. Hence, the Nusselt number is defined as

$$Nu = -\frac{k^*}{c_p}\frac{h_H - h_C}{T_H - T_C}\frac{\partial t}{\partial \xi}\bigg|_{wall} + Pr\,Gr^{0.5}\rho^* u \frac{h_A}{c_{pr}(T_H - T_C)} \quad (16)$$

or $Nu = (Q_d + Q_a)$ where Q_a is the dimensionless energy flux due to advection.

Similarly, the Sherwood number at the wall is the mass transfer over the mass transfer due to only diffusion in the cavity. In the absence of natural convection, the concentration field is diffusion dominated, and the Sherwood number is equal to unity. Hence, the Sherwood number illustrates the increased mass transfer (concentration gradient) at the wall due to natural convection effects

$$Sh = \frac{h_m H}{\rho_r D_{ABr}} = -\rho^* D^*_{AB}\frac{\partial \phi}{\partial \xi}\bigg|_{wall}. \quad (17)$$

If no mass transfer occurs at the wall, the Sherwood number vanishes (the concentration gradient would be zero).

Method of solution

The methodology used to solve equations (1)–(5) and the associated boundary conditions is based on the implicit, control volume, finite difference technique SIMPLER [19]. A non-uniform grid was employed for the finite-difference mesh. The nodes are closely spaced at the walls. The small control volume at the wall results in the four velocities at the control surfaces being the same order of magnitude. Hence, a better estimate of the velocity, temperature and concentration gradients is achieved which promotes overall energy and mass balances. A specified thickness of L at the vertical walls (or H for the horizontal walls) was divided into control volumes using a linear weighted average of a power law and linear spacing of the control volume surfaces.

A few other remarks need to be made regarding the numerical solution of the problem. Since species B is noncondensable, the enthalpy of the gas leaving and entering the cavity is that of species A only and not the mixture enthalpy which is the property conserved through the energy equation. The solution is taken to be converged when overall energy and mass balances are achieved (not more than 3% difference between hot and cold wall values), and the dependent field variables are not changing between consecutive iterations. In order to obtain an energy balance for the variable property cases, the energy balance was made in terms of the enthalpy, since it was the conserved dependent variable (not temperature). The temperature is determined in the following manner. The enthalpy at temperature T is evaluated from

$$h = \omega_A \int_0^T c_{pA}\,dT + (1-\omega_A)\int_0^T c_{pB}\,dT \quad (18)$$

(the enthalpy at 0 K is arbitrarily taken as zero). Since c_p is a function of temperature only (for an ideal gas), equation (18) can be rearranged after integration to solve for the temperature. This results in an implicit equation for the temperature (temperature is on both sides of the equation), and therefore must be solved iteratively.

Validation of numerical methodology

To gain confidence in the methodology, the computer program was used to solve for single component natural convection in a square cavity. The predictions based on the computer program used in this work were compared with the benchmark solution of de Vahl Davis [24]. Agreement between the benchmark solution and the values predicted from the program used in this work for u_{max}, w_{max}, $\overline{Nu}_H$ and $Nu_{H,max}$ is within 3% for a Rayleigh number of 1×10^4, 1×10^5 and 1×10^6. A non-uniform grid of 60×60 was used with the SIMPLER algorithm [19] for this comparison.

The grid independence of the results obtained using a finite-difference method of solution is of concern. The w-velocity, temperature and concentration distributions at $\zeta = 0.5$ were compared for natural convection in a binary gas ($Gr = 1\times10^5$, $N^* = -1.209$, $Pr = Sc = 1$, $M^* = 5$, $\Delta\omega_A = 0.3$, $\omega_C = 0$, $C_{wv} = 3.33$, $\Delta T = 37.7$ and $C_T = 7.5$) using grids of 35×35, 45×45 and 55×55 nodes. There is little difference in any of the dependent variable distributions. The number of nodes in the portion of the grid at the wall where the spacing is nonuniform (smaller mesh spacing) is 8, 11 and 13 for a 35×35, 45×45 and 55×55 mesh size, respectively. For all three grid sizes, the portion of the mesh containing the non-uniformly spaced nodes is $0.125H$ (or $0.125L$). The values used to begin the iterative solution procedure for the two smaller grids were interpolated from the solution obtained using the 55×55 node mesh. The larger number of nodes is helpful in obtaining a converged solution when the dimensionless parameters are changed, because the estimate of the dependent variable gradients is better. The 55×55 node finite-difference grid is used throughout the remainder of the numerical work. Further details can be found elsewhere [25].

RESULTS AND DISCUSSION

Buoyancy parameter

Invoking the Boussinesq approximation yields the buoyancy parameter, N, which is defined as [6]

$$N = \frac{\beta_C(\omega_H - \omega_C)}{\beta_T(T_H - T_C)} = \frac{\beta_C \Delta\omega_A}{\beta_T \Delta T} \quad (19)$$

where

$$\beta_T = \frac{1}{T_r} \quad \text{and} \quad \beta_C = \frac{M_B - M_A}{M_B\omega_{Ar} + M_A\omega_{Br}} = \frac{1 - M^*}{\omega_{Ar}(1 - M^*) + M^*}. \quad (20)$$

The ideal gas equation of state is assumed to be valid to obtain equation (20), and T_r is in absolute temperature. Note that if $M^* = 1$ or $\Delta\omega_A = 0$, $N = 0$ and the buoyancy force due to solutal gradients vanishes.

The variation of N with M^* and $\Delta\omega_A$ is shown in Fig. 2. The concentration difference across the cavity, $\Delta\omega_A$, varies from 0 to 1. The solutal and thermal buoyancy forces are augmenting for $N > 0$ and opposing for $N < 0$. For constant M^*, $|N|$ increases as $\Delta\omega_A$ increases, but the variation is not linear. The increase of $|N|$ with $\Delta\omega_A$ is less for $M^* < 1$ and greater for $M^* > 1$ compared to a linear variation. Therefore, increasing the amount of species A present in the cavity (due to $\Delta\omega_A$ becoming larger) results in the solutal body force augmenting the thermal body force at a decreasing rate, since $M_A < M_B$ ($M^* < 1$). Conversely, when $M_A > M_B$ ($M^* > 1$), increasing the amount of species A present results in the solutal body force opposing the thermal body force at an increasing rate.

Without making the Boussinesq approximation, the body force can be rearranged to yield the buoyancy parameter as given in equation (3)

$$N^* = \frac{\rho_C - \rho_H}{\rho_r \beta_T \Delta T} \quad (21)$$

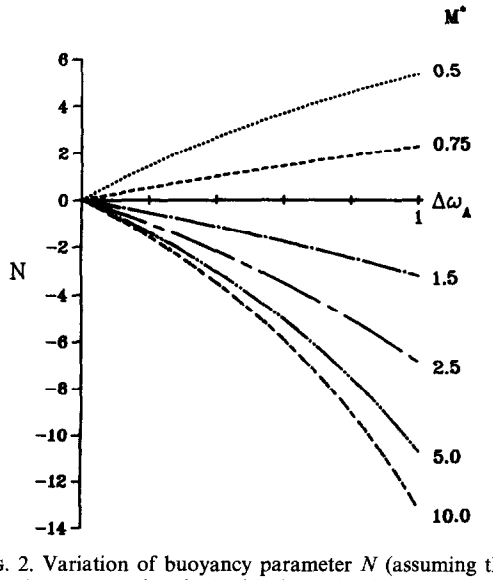

FIG. 2. Variation of buoyancy parameter N (assuming the Boussinesq approximation) with the molecular weight ratio and concentration difference across the cavity.

where ρ_r is the reference density evaluated at the reference temperature and concentration (average of hot and cold wall values of temperature and concentration). The reference density is not equal to $(\rho_C + \rho_H)/2$. Since $\beta_T \Delta T$ is always positive, the sign of N^* is manifested through $(\rho_C - \rho_H)$. For flow down along the hot wall (opposing buoyancy forces) $\rho_H > \rho_C$ and N^* is negative. Note that if $\Delta\omega_A = 0$ or $M^* = 1$, equation (21) reduces to

$$N^* = \frac{(0.5 + C_T)^2}{(C_T + C_T^2)} \quad (22)$$

which is approximately equal to one (except for small values of C_T) and is a function of temperature only (buoyancy effects due to solutal differences vanish). For $\Delta\omega_A = 0$ or $M^* = 1$, as C_T becomes large (ΔT becomes small), $N^* = 1$, and temperature variations do not affect N^*. The variation of N^* is similar to that for N, but is much more nonlinear. Furthermore, all values of $N^* > 1$ denote that the thermal and solutal buoyancy forces augment one another, and for $N^* < 1$ the two buoyancy forces oppose each other. If $N^* = 0$, the total body force vanishes independent of the Prandtl and Schmidt number (in contradistinction to the constant property case with $N = -1$).

Variable thermophysical property effects

The large number of parameters involved in this study (M_A, M_B, pure component thermophysical property variation with temperature for species A and B and the variation of thermophysical properties with concentration) result in an analysis which is hard to generalize. Different species were chosen to model pure component property ratios as being more representative of a physical system. The intent of this work is to show typical results of thermophysical property variations for specific binary mixtures rather than to consider many cases illustrating the effects of a particular property. The authors believe that it is inappropriate to isolate a single thermophysical property and account for its variation while maintaining the remaining properties constant. Therefore, the thermophysical properties of argon, nitrogen and ethanol were used in this parametric study. The properties are well defined and future experiments could easily use these gases.

The thermophysical property variations designated by 1, 2 and 3 are those of ethanol, nitrogen and argon, respectively [26–28], except for the specific heat of ethanol. The specific heat of gas 1 is given by $c_p = A + BT + CT^2 + DT^3$, where $A = 0.131122$, $B = 9.18566\text{E}-04$, $C = -2.35957\text{E}-07$ and $D = -7.19165\text{E}-11$ with T in K and c_p in cal g^{-1} K^{-1} [27]. This anomaly occurs because two newer references [29, 30] for the specific heat of ethanol which are consistent (found after the parametric study was completed) gave significantly different values of c_p from that used for gas 1. This anomaly is of little

consequence, since the parametric study is intended to show trends and not to represent any particular material characteristic. Furthermore, the fact that the thermophysical property variations are used for a particular temperature range is not restrictive. Since the thermophysical properties are given as dimensionless ratios, the results are indicative of any temperature range over which the properties would vary in the manner given. In addition, the values of the thermophysical properties are not used since the equations are expressed in terms of the dimensionless property ratios. Even the term $(h_H - h_C)/c_{pr}(T_H - T_C)$ contains a specific heat ratio implicitly. Mixture properties are determined using the Gibbs–Dalton law for ideal gases [31] and the Chapman–Enskog theory [23] for mixtures of gases at low density.

The base case 1v is denoted by $Gr = 1 \times 10^5$, $Sc = Pr = 1.0$, $N^* = -1.209$, $M^* = 5.0$, $\Delta\omega_A = 0.3$, $\omega_C = 0.0$, $\Delta T = 37.7$ K and $T_C = 283.15$ K. Lower case v and c refer to variable and constant thermophysical property cases, respectively. Table 1 lists the parameters of the cases examined in this study. The values of N^*, $\Delta\omega_A$, M^*, ω_{AC} and C_{wv} are consistent with equation (21). In other words, equation (21) equates N^* to a function of $\Delta\omega_A$ which makes it more convenient to select integer values of $\Delta\omega_A$ and use the resulting non-integer value of N^* [25]. In some instances, more than one parameter must be changed to maintain consistency. For example, changing $\Delta\omega_A$ affects both N^* and C_{wv}. Tables 2 and 3 list, respectively, the hot and cold wall average values of the mass flux ($\rho^* u$), Nusselt number (Nu), energy flux due to advection and diffusion (Q_a and Q_d) and the Sherwood number (Sh). For example, the average of any parameter, Φ, is defined as

$$\bar{\Phi} = \frac{1}{H}\int_0^H \Phi \, dz = \int_0^1 \Phi \, d\zeta. \tag{23}$$

The integral is evaluated numerically.

Base case. The results for the base case (case 1v) are given in Fig. 3 as contour plots of the streamlines, temperature, mixture thermal conductivity and mixture density. Isolines of the thermophysical properties are given as a representative example of thermophysical property variation. The concentration refers to the mass fraction of species A which will be used consistently. The velocity, enthalpy, temperature and thermophysical properties are those of the mixture. Since N^* is negative, the solutal buoyancy force dominates and opposes the thermal buoyancy force. Hence, flow is down along the hot wall and up along the cold wall as anticipated. The mass transfer at the hot and cold walls introduces an appreciable mass flow into the cavity as seen from the streamlines of Fig. 3(a). This results in a blowing and suction effect on the velocity, temperature and concentration gradients at the hot and cold wall, respectively. The thermophysical property variation across the cavity is significant and is due mainly to the concentration gradient. For example, the thermal conductivity increases with temperature for a pure gas, but the mixture thermal conductivity is largest at the cold wall, because k_A is smaller than k_B (in this case), and the mass fraction of species A decreases from the hot to the cold wall.

The local heat and mass transfer at the hot and cold walls for case 1v is shown in Fig. 4. The distribution of advective energy flux at the hot wall is identical (in shape, not magnitude) to the u-velocity distribution at the wall since ρ and h_A are constant at the hot wall where mass enters the cavity. At the cold wall, ρ and h_A leaving the cavity are nearly constant such that the distribution of Q_{aC} (where subscript C denotes a value with respect to the cold wall) is practically representative of the u-velocity distribution at the wall. The energy and mass fluxes at the hot and cold walls are largest at the top and bottom of the cavity, respectively, due to the reversed flow (as compared to natural convection in a single component fluid). The temperature and mass fraction gradients are largest where the horizontal flow impinges upon the hot or cold wall. The advected energy flux is the greater portion of the total energy flux at both vertical walls, but is a smaller fraction of the total at the cold wall (as compared to the hot wall) due to the variation of thermophysical properties. The average mass flux at the hot wall is equal to the average mass flux out at the cold wall, but $h_{AH} > h_{AC}$.

Further insight into the effect of variable properties on the flow and heat and mass transfer can be gained by comparing the results with those obtained by assuming constant thermophysical properties. Direct comparison is not possible because of the different body force terms. A reasonable comparison can be made if an averaged value of N is used in the constant thermophysical property case. A value of N is determined at the hot and cold wall. The average of these two values results in $N = N^* - 1$ for comparison of results for constant and variable thermophysical property cases.

For constant thermophysical properties with $Pr = Sc = 1$, the temperature and concentration fields are identical, and the diffusive energy and mass fluxes at the wall are the same. There are noticeable differences in the contours of streamlines, temperature and concentration between the results for constant and variable properties, but surprisingly there is little difference between the local Sherwood (Sh) and Nusselt (Nu) numbers for constant and variable property cases at either the hot or cold walls. This is due to the property variations. The mass flux at the walls increased slightly, but h_A is less than $c_{pr}T$ (constant property case) at the cold wall such that Q_a for case 1v increases and decreases at the hot and cold wall, respectively, as compared to case 1c (Tables 2 and 3). Also, the enthalpy gradient is decreased and increased at the hot and cold wall, respectively, due partially to the increase in mass flux at the walls. Considering diffusion heat transfer alone with $(k^*/c_p^*)_H < (k^*/c_p^*)_C$,

Table 1. Range of parameters examined in the numerical study with variable properties

Case	Gr	Pr	Sc	N^*	Species A	Species B	M^*	$\Delta\omega_A$	ω_C	C_{wv}	ΔT (K)	C_T	$\frac{c^*_{pH}}{c^*_{pC}}$	$\frac{k^*_H}{k^*_C}$	$\frac{\mu^*_H}{\mu^*_C}$	$\frac{\rho^*_H}{\rho^*_C}$
1v	1×10^5	1.0	1.0	−1.209	1	2	5.0	0.3	0.0	3.33	37.7	7.5	1.09 / 0.92	0.92 / 1.08	0.90 / 1.09	1.09 / 0.94
4v						3							1.26 / 0.76	0.94 / 1.07	0.89 / 1.10	1.09 / 0.94
5v					2	1							0.97 / 1.02	1.05 / 0.92	1.00 / 1.00	1.09 / 0.94
9v				−0.514							56.6	5.0	1.10 / 0.92	0.94 / 1.05	0.92 / 1.06	1.06 / 0.97
10v							2.5	0.4		2.50			1.12 / 0.90	0.83 / 1.25	0.80 / 1.26	1.09 / 0.94
11v				−1.721					0.2	2.67			1.09 / 0.92	0.91 / 1.09	0.89 / 1.11	1.13 / 0.91

Table 2. Summary of the average mass flux, Nusselt number, energy flux due to advection and diffusion and Sherwood number at the hot wall

Case	$\overline{\rho^* u}\times10^3$	$\overline{Nu}$	$\overline{Q}_a$	$\overline{Q}_d$	$\overline{Sh}$
1v	5.61	18.58	15.12	3.46	4.14
4v	5.54	25.19	24.56	0.63	4.09
5v	5.59	14.73	10.27	4.46	4.13
9v	4.38	11.25	8.53	2.72	3.23
10v	8.12	24.32	21.35	2.97	3.85
11v	8.32	24.11	20.39	3.72	4.39
1c	5.38	18.42	14.45	3.97	3.97
2c	5.48	18.80	14.74	4.05	4.04

Table 3. Summary of the average mass flux, Nusselt number, energy flux due to advection and diffusion and Sherwood number at the cold wall

Case	$\overline{\rho^* u}\times10^3$	$\overline{Nu}$	$\overline{Q}_a$	$\overline{Q}_d$	$\overline{Sh}$
1v	5.53	18.57	12.42	6.15	5.83
4v	5.54	25.03	20.43	4.61	5.84
5v	5.60	14.64	9.07	5.56	5.90
9v	4.36	11.35	6.50	4.84	4.60
10v	8.01	24.21	17.54	6.67	6.33
11v	8.22	23.93	16.76	7.17	6.93
1c	5.40	18.51	12.81	5.69	5.69
2c	5.50	18.85	13.07	5.78	5.80

the enthalpy gradient increases and decreases at the hot and cold wall, respectively (maintaining a constant diffusive heat flux). But the larger enthalpy gradient at the hot wall, for example, is multiplied by a smaller diffusion coefficient, which results in a smaller change in the diffusive heat flux. The resulting effect of increased advective and decreased diffusive energy fluxes is a slight increase in $\overline{Nu}_H$. The Sherwood number increased at both walls since the circulation in the cavity intensified, which increased the concentration gradient. Case 2c is the same as case 1c, except the buoyancy term is defined using the density (the Boussinesq approximation is not made). In other words, the buoyancy term is the same as that for the variable properties case. The diffusive energy and mass fluxes at both walls have increased due to the increased circulation in the cavity. In particular, comparison of case 1v with case 2c in Tables 2 and 3 illustrates that the decrease in the diffusion coefficient decreases the diffusive energy flux at the hot wall.

An interesting result owing to the variation of properties with temperature and concentration is that the recirculation cells have shifted more to the lower half of the cavity for the variable properties case (Fig. 3(a)). Correspondingly, the streamlines are closer together (which implies the mass flux is higher since the flow, $\rho^* u$, between any two streamlines is constant). Figure 5 illustrates the velocity dis-

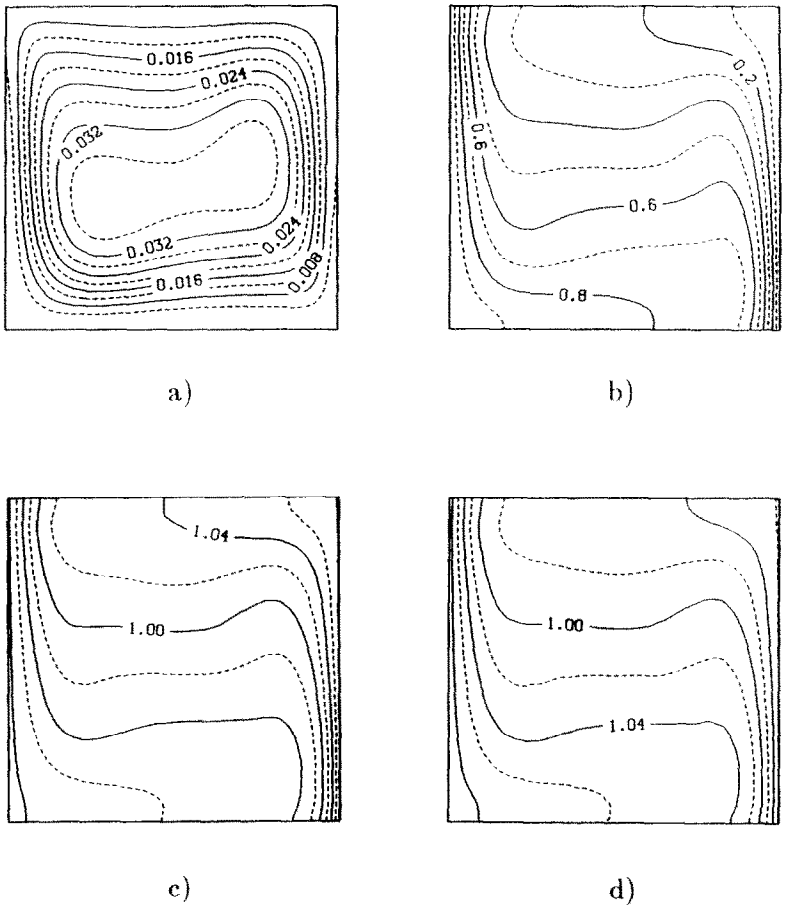

FIG. 3. Streamline contours (a) for the base case 1v ($Gr = 1 \times 10^5$, $Sc = Pr = 1.0$, $N^* = -1.209$, $M^* = 5.0$, $\Delta\omega_A = 0.3$, $\omega_C = 0.0$, $\Delta T = 37.7$ K and $T_C = 283.15$ K) and isolines of the temperature (b), mixture thermal conductivity (c) and mixture density (d).

tributions for cases 1v and 1c at the centerline ($\xi = 0.5$) and midheight ($\zeta = 0.5$). The maximum velocities for the variable property case are: $u = 0.152$ and -0.092, $w = 0.255$ and -0.255; for the constant property case, they are: $u = 0.118$ and -0.111, $w = 0.242$ and -0.254.

The ξ-momentum is a balance between inertia and viscous forces, with the ζ-momentum additionally influenced by the buoyancy force. Furthermore, continuity of mass must be satisfied. The u-velocity distribution exemplifies the combined effects of conserving mass and momentum. For constant prop-

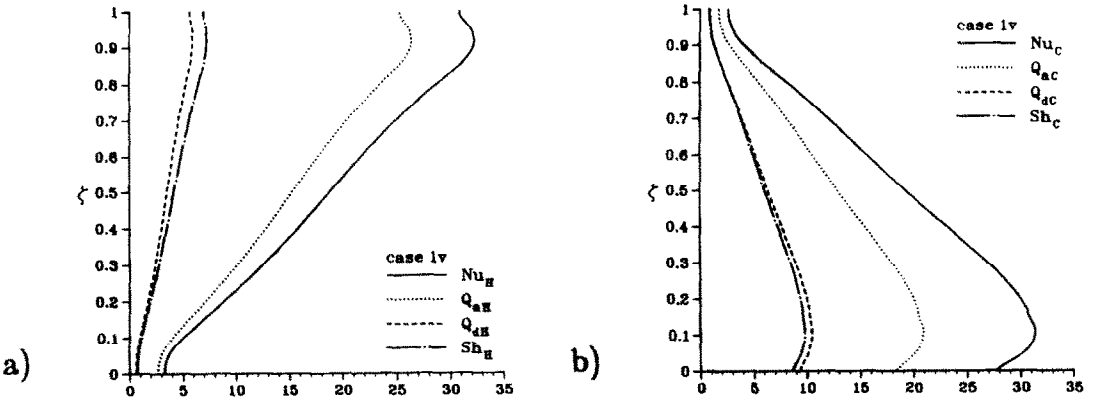

FIG. 4. Variation of the Nusselt number, energy flux due to advection and diffusion and Sherwood number (base case 1v: $Gr = 1 \times 10^5$, $Sc = Pr = 1.0$, $N^* = -1.209$, $M^* = 5$, $\Delta\omega_A = 0.3$, $\omega_C = 0$, $\Delta T = 37.7$ K and $T_C = 283.15$ K) at the hot wall (a) and cold wall (b).

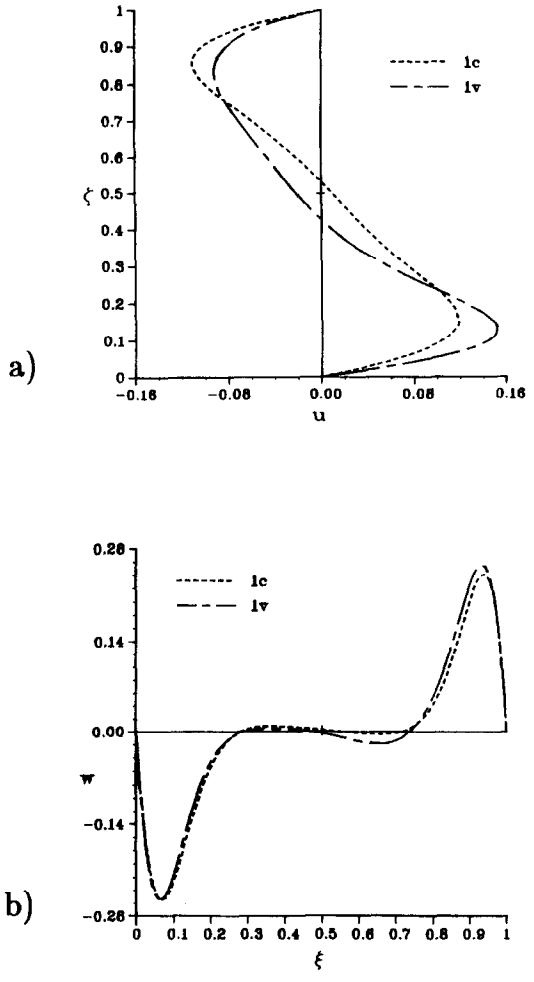

FIG. 5. Comparison of velocity distributions from the base case 1v ($Gr = 1 \times 10^5$, $N^* = -1.209$, $Pr = Sc = 1.0$, $M^* = 5$, $\Delta\omega_A = 0.3$, $\omega_C = 0$, $\Delta T = 37.7$ K and $T_C = 283.15$ K) and case 1c (constant properties: $Gr = 1 \times 10^5$, $Pr = Sc = 1.0$ and $N = -2.209$) of the u-velocity at $\xi = 0.5$ (a) and of the w-velocity at $\zeta = 0.5$ (b).

erties, the flow in the positive ξ-direction takes place over more than half the cavity. This occurs because mass is added and removed at the hot and cold wall, respectively. Mass addition at constant density must increase either the velocity or the area across which the fluid passes to maintain continuity of mass (the maximum positive u-velocity is only slightly larger than the maximum negative u-velocity). In contrast for variable properties, the flow in the positive ξ-direction occurs over less than half of the cavity. Note that $\rho_H > \rho_C$ and $\mu_H < \mu_C$. Fluid at the hot and cold walls is advected (in this case) along the bottom and top walls, respectively. The thermophysical properties are functions of the local temperature and mass fraction of the fluid. For constant shear at the wall, decreasing μ increases u (assuming everything else remains the same). Therefore, $|u|$ is greater at the bottom wall than at the top. Combined with the density being larger at the bottom connecting wall than at the top, the area across which the fluid passes in the positive ξ-direction is smaller than that of the flow area in the negative ξ-direction.

The w-velocity distributions for the constant and variable property cases are very similar. The velocity distributions in the core of the cavity are different since the circulation is greater for case 1v. The addition and removal of mass at the walls accounts for the difference in the peak velocities for the constant property case. There are three effects which can be attributed to the similarity between the variable and constant property cases. For example, consider the cold wall. First, $\mu_C > \mu_H$. This results in the velocity gradient at the cold wall being smaller as compared to case 1c (for constant shear). Secondly, since the mass flux increased, the suction effect on the boundary layer at the cold wall increases. This increases the velocity gradient at the cold wall. Finally, $(\rho_r - \rho_C)/(\rho_H - \rho_C)$ is less than 0.5. Therefore, the buoyancy force at the cold wall has decreased as compared to the constant property case. The second effect opposes the first and third.

From these arguments, the velocity, temperature and concentration gradients at the wall result from the interaction of advective and diffusive forces, thermophysical property variation with temperature and concentration, and the mass flux at the walls (when the normal velocity at the wall is appreciable). Typically, a change in one dependent variable is accompanied by the alteration of another variable which may augment or oppose the influence of the first.

Effects of thermophysical property differences between components. The effects of variable thermophysical properties are further investigated in cases 4v and 5v. For case 4v, species B is represented by gas 3 (argon, c_{pB} and k_B decrease and μ_B increases as compared to the base case). The variation of the mixture specific heat has increased as compared to the base case along with the thermal conductivity variation decreasing slightly. This results in the reduction of the diffusive energy flux (Tables 2 and 3). The relatively low value of $\overline{Q_{dH}}$ results from Q_d decreasing more at the hot wall and $\overline{Q_{dH}}$ being less than $\overline{Q_{dC}}$ (compare the decrease of $\overline{Q_{dC}}$ and $\overline{Q_{dH}}$ from case 1v to case 4v). The total energy flux is increased, because the enthalpy of species A entering and leaving the cavity is larger (c_{pA}/c_{pB} increased) compared to the enthalpy of species B which results in Q_a being larger (Fig. 6). This also results in a region of slightly negative dimensionless temperature (not shown for the sake of brevity). The negative θ signifies that the fluid temperature is smaller than the cold wall temperature. Only species A is removed from the cavity at the cold wall. Since species A carries the greater fraction of the energy content of the mixture as compared to the base case, the mixture enthalpy is reduced, although the concentration is nearly the same. With reduced enthalpy for nearly the same mass fraction, the temperature decreases. The maximum temperature

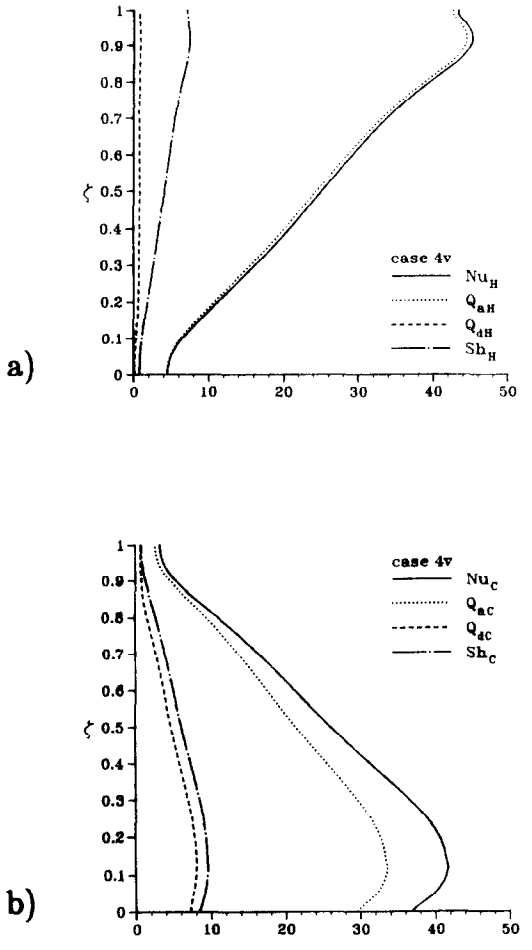

FIG. 6. Effect of different thermophysical properties (case 4v: species A—ethanol, species B—argon) on the Nusselt number, energy flux due to advection and diffusion and Sherwood number at the hot wall (a) and cold wall (b).

decrease below the wall temperature is 0.5°C (1.3% of ΔT). Accounting for the difference between the enthalpy of the fluid leaving or entering the cavity at the wall (as being that of species A only) and the mixture enthalpy is actually accounting for species interdiffusion, but only at the wall. In a companion paper [32] dealing with species interdiffusion and Soret and Dufour effects, the previously discussed effect is more pronounced.

The thermophysical properties of species A and B for the base case are transposed for case 5v. In this situation, the variation due to temperature opposes that due to concentration for the specific heat (c_{pA} is constant and c_{pB} increases with temperature in regions where ω_B decreases). As such, the variation of the specific heat of the mixture is about 30% of that of the base case. Moreover, the specific heat is greatest at the cold wall for case 5v. The thermal conductivity is greater at the hot wall in this case, with the magnitude of the variation across the cavity being similar to that for the base case. In contrast, the viscosity varies very little, although the viscosity is greatest at the hot wall. This is due to the characteristics of gases 1 and 2 [25]. Since the variation of c_p and k are reversed from the base case, the diffusive heat flux for case 5v has increased and decreased at the hot and cold walls, respectively (Tables 2 and 3). The advective energy flux at both walls decreased because c_{pA}/c_{pr} decreased. Hence, the total energy ($\bar{N}u$) transferred at the walls is decreased.

Do not confuse the ratios of the pure component thermophysical properties (e.g. k_A/k_B) with the variation of the mixture thermophysical properties (or mixture property ratios, e.g. k_H^*/k_C^*) which depend on the concentration and temperature fields and variation of pure component thermophysical properties. For example, assuming constant thermophysical properties for the mixture and reversing species A and B would result in a change of the average (or reference) mixture thermophysical properties which influence the Pr, Sc and Ra only. However, reversing species A and B of a binary system with variable thermophysical properties (case 5v, for example) would result not only in the same change of reference mixture properties (change in Ra, Pr and Sc), but also in the variation of the thermophysical properties across the cavity in the opposite direction (as compared to case 1v). This would result in the change of the tabulated values, since Pr, Sc and Ra were not changed.

Velocity distributions for cases 1v, 4v and 5v are shown in Fig. 7. In particular for case 5v, the peak u-velocity has decreased as compared to the base case, because the viscosity is larger for case 5v as compared to the base case. For constant shear at the wall, increased viscosity decreases the velocity. Since the velocity decreases, the area across which the fluid flows (in the positive ξ-direction) increases for a constant mass flow rate. For case 4v, the viscosity has decreased in the lower half of the cavity which increases the velocity (with everything else constant). Note, that the w-velocity at $\zeta = 0.5$ is practically the same for all three cases. Since the buoyancy force and the mass flux at the walls for all three cases are nearly equal, the change in viscosity does not affect the velocity distribution at the midheight of the hot and cold walls. Hence, the balance between inertia and buoyancy forces dominate the flow (although the viscous effects are not negligible).

A comparison of the local Nusselt and Sherwood numbers (Fig. 8) for different thermophysical properties (cases 1v, 4v and 5v) indicates that the thermophysical properties significantly influence the temperature gradients at the wall (as discussed), but affect the concentration gradients very little. The concentration gradient is influenced by the density and mass diffusion coefficient (which depends on the temperature). Since ρ^* and D_{AB}^* are the same for cases 1v, 4v and 5v at the wall (ω_A and T are the same at the wall for all three cases), the Sherwood number is affected very little.

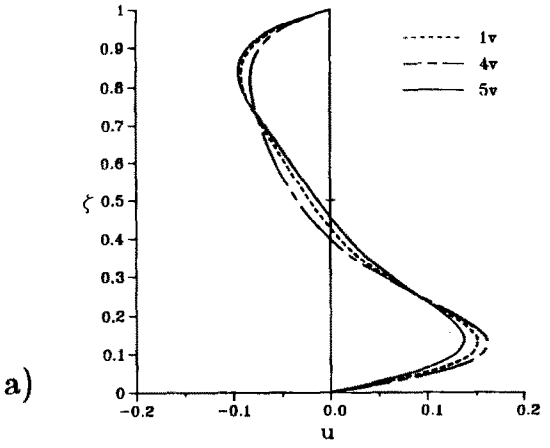

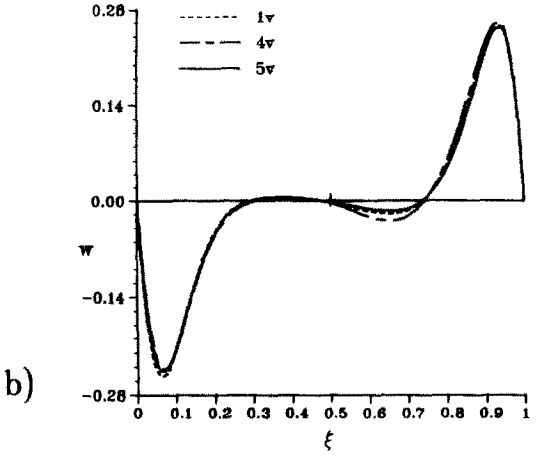

FIG. 7. Effect of different thermophysical properties (base case 1v: A—ethanol, B—nitrogen; case 4v: A—ethanol, B—argon; case 5v: A—nitrogen, B—ethanol) on the u-velocity at $\xi = 0.5$ (a) and w-velocity at $\zeta = 0.5$ (b).

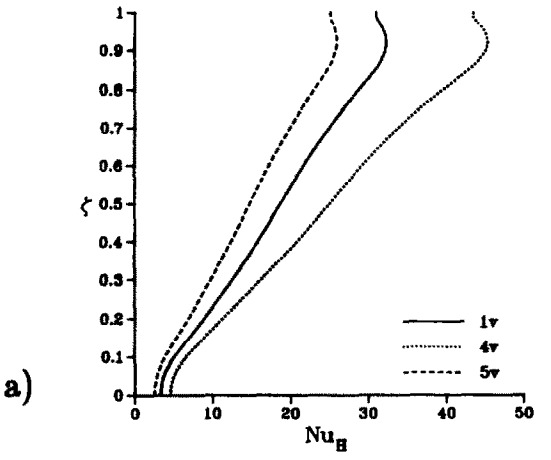

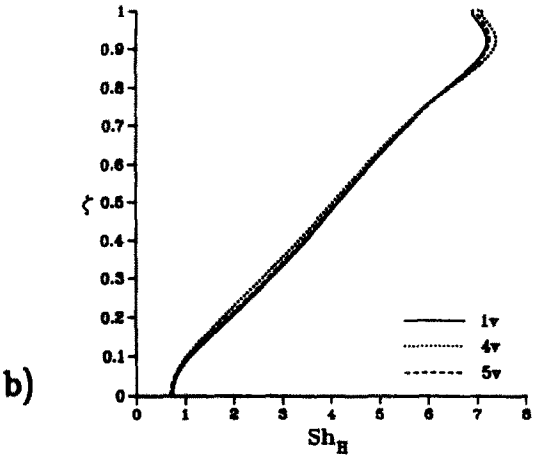

FIG. 8. Effect of different thermophysical properties (base case 1v: A—ethanol, B—nitrogen; case 4v: A—ethanol, B—argon; case 5v: A—nitrogen, B—ethanol) on the hot wall Nusselt number (a) and Sherwood number (b).

Effects of the temperature and concentration difference across the cavity. For case 9v, an increase of ΔT across the cavity reduces N^* and decreases the circulation in the cavity (Fig. 9(b)). The greater temperature difference makes the temperature dependence of the properties more important. The specific heat (and mass diffusivity) varies more and the thermal conductivity, viscosity and density vary less as compared to the base case. The decreased thermal conductivity and increased specific heat reduce the diffusive energy flux at the wall. Moreover, the advection at the wall is also reduced, since $\rho^* u$ decreased (Tables 2 and 3). Correspondingly, the local Nusselt and Sherwood numbers also decrease as shown in Fig. 10.

Case 10v has the same N^* as the base case but the molecular weight ratio and concentration difference across the cavity are different. Also, C_{wv} is different since $\Delta\omega_A$ has become larger. Because C_{wv} decreased, the velocity normal to the wall increased. This intensifies the circulation in the cavity (Fig. 9(c)). The variation of the mixture specific heat, thermal conductivity and viscosity increased. In contrast, the density changed little. This occurs because the decrease in M^* is offset by the increase in $\Delta\omega_A$. An increase in the thermal conductivity and mass flux out of the cavity and a decrease in the specific heat enhance the temperature and concentration gradients at the cold wall. Conversely, an increase in the mass flux into the cavity and specific heat and a decrease in the thermal conductivity reduce the temperature and concentration gradients at the hot wall. Hence, the average Nusselt and Sherwood numbers increase at the cold wall and decrease at the hot wall as compared to the base case.

Case 11v has the same concentration difference across the cavity as the base case, but with $\omega_C = 0.2$. This reduces C_{wv} (increases the normal velocity at the hot and cold walls) and makes N^* larger, which intensifies the circulation in the cavity (Fig. 9(d)).

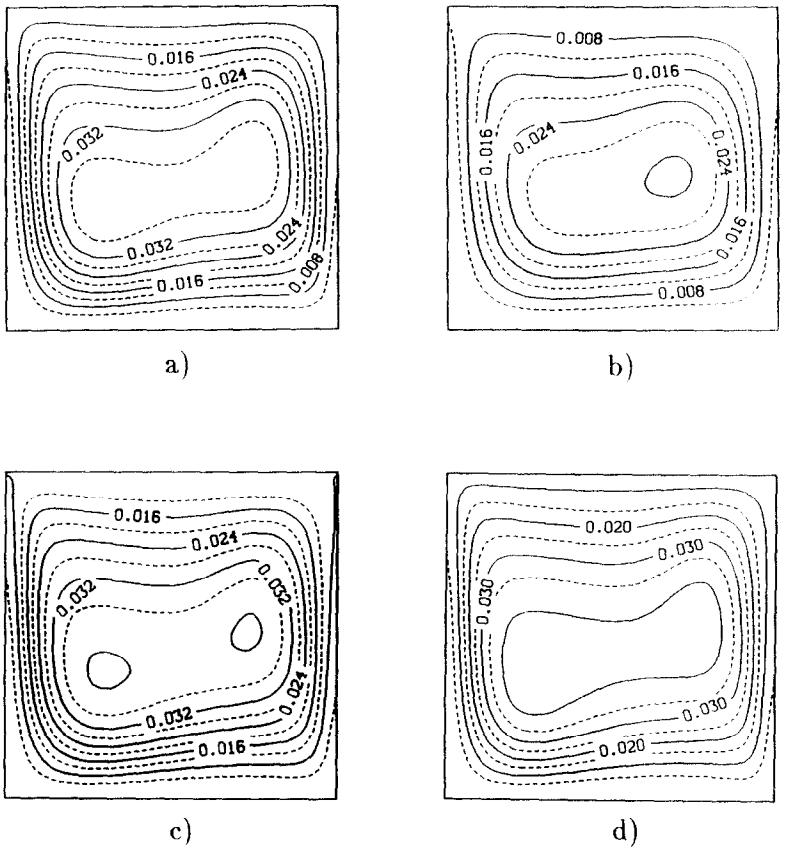

FIG. 9. Comparison of streamline contours for different temperature and concentration differences across the cavity: (a) $\Delta T = 37.7$ K, $N^* = -1.209$, $\Delta\omega_A = 0.3$, $\omega_C = 0.0$, $C_{wv} = 3.33$, $M^* = 5.0$ (base case 1v), (b) $\Delta T = 56.6$ K, $N^* = -0.514$ (case 9v), (c) $\Delta\omega_A = 0.4$, $C_{wv} = 2.5$, $M^* = 2.5$ (case 10v) and (d) $N^* = -1.721$, $\omega_C = 0.2$, $C_{wv} = 2.67$ (case 11v).

Note the variation of the specific heat is nearly the same as for the base case, because the mass fraction difference $\Delta\omega_A$ is the same. The absolute values of the specific heat for the two cases are different since species A contributes more to the mixture specific heat for case 11v. The dimensionless advective energy flux decreases since the enthalpy of species A at the vertical walls is the same, but the mixture enthalpy has become larger. The variation of the thermal conductivity is approximately the same, but the variation of the vis-

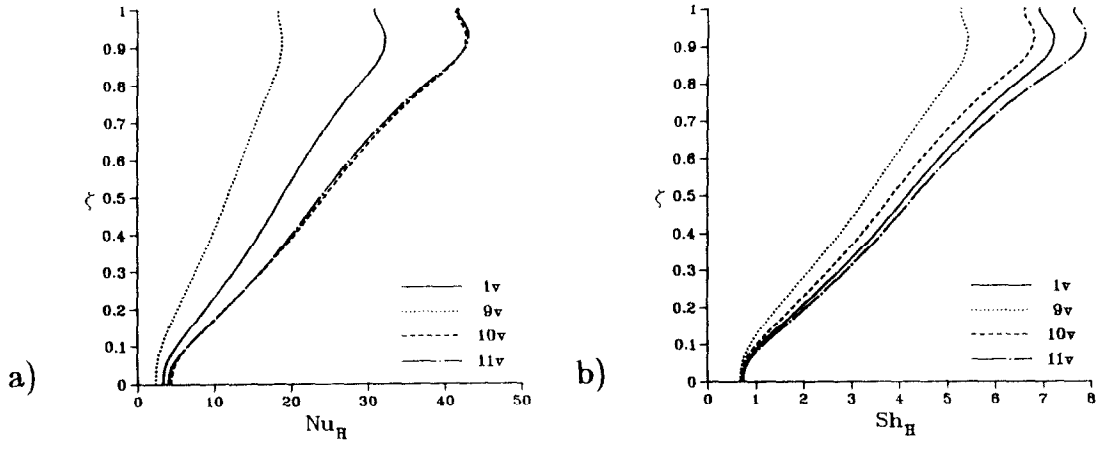

FIG. 10. Effect of the temperature and concentration difference across the cavity (base case 1v: $\Delta T = 37.7$ K, $N^* = -1.209$, $\Delta\omega_A = 0.3$, $\omega_C = 0.0$, $C_{wv} = 3.33$, $M^* = 5.0$; case 9v: $\Delta T = 56.6$ K, $N^* = -0.514$; case 10v: $\Delta\omega_A = 0.4$, $C_{wv} = 2.5$, $M^* = 2.5$; case 11v: $N^* = -1.721$, $\omega_C = 0.2$, $C_{wv} = 2.67$) on the hot wall Nusselt number (a) and Sherwood number (b).

cosity is significantly greater as compared to the base case. Furthermore, the variation of the density has increased as expected since N^* has become larger.

CONCLUSIONS

In this paper, an analysis and results describing variable thermophysical property effects on natural convection with simultaneous heat and mass transfer across a cavity are presented. The Boussinesq approximation is inappropriate as the molecular weight ratio of species A to species B (M^*) differs from one. The thermophysical properties vary significantly due to differences in concentration (depends on M^* and the pure component thermophysical properties). The variation of the thermophysical properties due to temperature may either aid or oppose that due to concentration. Variation of thermophysical properties results in different velocity, temperature and concentration gradients at the hot and cold walls. Furthermore, the mass flux into the cavity at the hot wall and out of the cavity at the cold wall decreases and increases, respectively, the velocity, temperature and concentration gradients at the vertical walls due to blowing and suction effects. For example, $Q_{dH} < Q_{dC}$ due to the thermophysical properties and mass flux at the vertical walls (case 1v). For case 5v, the thermophysical property variation for species A and B are reversed from case 1v. This results in the mixture specific heat varying less across the cavity, and the mixture thermal conductivity being largest at the hot wall for case 5v (for case 1v, the mixture specific heat and thermal conductivity are largest at the cold wall). Hence, Q_{dC} and Q_{dH} are closer in magnitude, but Q_{dC} remains larger due to the mass flux at the vertical walls.

Acknowledgements—One author (J.A.W.) is grateful for the financial support provided by a NASA Graduate Student Researchers Fellowship, under Grant NGT-50207. In addition, the authors would like to thank Prof. Satish Ramadhyani for providing the numerical algorithm and for many helpful discussions concerning the computer program. Computational facilities provided by Purdue University's Computing Center are also appreciated.

REFERENCES

1. S. Ostrach, Natural convection in enclosures. In *Advances in Heat Transfer* (Edited by J. P. Hartnett and T. F. Irvine, Jr.), Vol. 8, pp. 161–227. Academic Press, New York (1972).
2. S. Ostrach, Natural convection heat transfer in cavities and cells. In *Heat Transfer—1982* (Edited by U. Grigull, E. Hahne, K. Stephan and J. Straub), Vol. 1, pp. 365–379. Hemisphere, Washington, DC (1982).
3. I. Catton, Natural convection in enclosures. In *Heat Transfer—1978*, Vol. 6, pp. 13–31. Hemisphere, Washington, DC (1978).
4. I. Catton, A. Bejan, R. Grief and K. G. T. Hollands, Natural convection in enclosures. In *Proceedings of a Workshop on Natural Convection* (Edited by K. T. Yang and J. R. Lloyd), pp. 24–35. University of Notre Dame, Notre Dame, Indiana (1982).
5. B. Gebhart, Y. Jaluria, R. L. Mahajan and B. Sammakia, *Buoyancy-induced Flows and Transport*. Hemisphere, New York (1988).
6. S. Ostrach, Natural convection with combined driving forces, *PhysicoChem. Hydrodyn.* **1**, 233–247 (1980).
7. M. M. Faktor and I. Garrett, *Growth of Crystals from the Vapor*. Wiley, New York (1974).
8. F. Rosenberger, *Fundamentals of Crystal Growth I—Macroscopic Equilibrium and Transport Concepts* (Edited by M. Cardonna, P. Fulde and H. Queisser), Springer Series in Solid State Sciences, Vol. 5. Springer, New York (1979).
9. F. Rosenberger, Fluid dynamics in crystal growth from vapors, *PhysicoChem. Hydrodyn.* **1**, 3–26 (1980).
10. F. Rosenberger, Convection in vapor crystal growth ampoules. In *Convective Transport and Instability Phenomena* (Edited by J. Zierep and H. Oertel), pp. 469–489. G. Braun, Karlsruhe (1982).
11. S. Ostrach, Fluid mechanics in crystal growth—The 1982 Freeman Scholar Lecture, *J. Fluids Engng* **105**, 5–20 (1983).
12. G. H. Westphal, Convective transport in vapor growth systems, *J. Crystal Growth* **65**, 105–123 (1983).
13. D. W. Greenwell, B. L. Markham and F. Rosenberger, Numerical modeling of diffusive physical vapor transport in cylindrical ampoules, *J. Crystal Growth* **51**, 413–425 (1981).
14. B. S. Jhaveri, B. L. Markham and F. Rosenberger, On singular boundary conditions in mass transfer across rectangular enclosures, *Chem. Engng Commun.* **13**, 65–75 (1981).
15. B. S. Jhaveri and F. Rosenberger, Expansive convection in vapor transport across horizontal rectangular enclosures, *J. Crystal Growth* **57**, 57–64 (1982).
16. B. L. Markham and F. Rosenberger, Diffusive-convective vapor transport across horizontal and inclined rectangular enclosures, *J. Crystal Growth* **67**, 241–254 (1984).
17. P. Ranganathan and R. Viskanta, Natural convection in a square cavity due to combined driving forces, *Numer. Heat Transfer* **14**, 35–59 (1988).
18. O. V. Trevisan and A. Bejan, Combined heat and mass transfer by natural convection in a vertical enclosure, *J. Heat Transfer* **109**, 104–112 (1987).
19. S. V. Patankar, *Numerical Heat Transfer and Fluid Flow*. Hemisphere, Washington, DC (1980).
20. W. T. Lai and J. W. Ramsey, Natural heat and mass transfer in a rectangular enclosure. In *Natural Circulation* (Edited by J. H. Kim and Y. H. Hassan), HTD-Vol. 92, pp. 361–372. ASME, New York (1987).
21. H. K. Wee, R. B. Keey and M. J. Cunningham, Heat and moisture transfer by natural convection in a rectangular cavity, *Int. J. Heat Mass Transfer* **32**, 1765–1778 (1989).
22. D. M. Kim and R. Viskanta, Heat transfer by conduction, natural convection and radiation across a rectangular cellular structure, *Int. J. Heat Fluid Flow* **5**, 205–213 (1984).
23. R. B. Bird, W. E. Stewart and E. N. Lightfoot, *Transport Phenomena*. Wiley, New York (1960).
24. G. de Vahl Davis, Natural convection of air in a square cavity: a bench mark numerical solution, *Int. J. Numer. Meth. Fluids* **3**, 249–264 (1983).
25. J. A. Weaver, Natural convection in binary gases with simultaneous heat and mass transfer across a cavity, Ph.D. Thesis, Purdue University, West Lafayette, Indiana (1989).
26. Y. S. Touloukian, P. E. Liley and S. C. Saxena, *Thermophysical Properties of Matter*, Vol. 3. Plenum, New York (1970).
27. Y. S. Touloukian and T. Makita, *Thermophysical Properties of Matter*, Vol. 6. Plenum, New York (1970).
28. Y. S. Touloukian, S. C. Saxena and P. Hestermans,

Thermophysical Properties of Matter, Vol. 11. Plenum, New York (1975).
29. R. C. Reid, J. M. Prausnitz and T. K. Sherwood, *The Properties of Gases and Liquids*. McGraw-Hill, New York (1987).
30. C. L. Yaws, H. M. Ni and P. Y. Chiang, Heat capacities for 700 compounds, *Chem. Engng* **95**, 91–98 (1988).
31. K. Wark, *Thermodynamics*, 3rd Edn. McGraw-Hill, New York (1977).
32. J. A. Weaver and R. Viskanta, Natural convection due to horizontal temperature and concentration gradients—2. Species interdiffusion, Soret and Dufour effects, *Int. J. Heat Mass Transfer* **34**, 3121–3133 (1991).

CONVECTION NATURELLE DUE A DES GRADIENTS HORIZONTAUX DE TEMPERATURE ET DE CONCENTRATION—1. EFFETS DES PROPRIETES THERMOPHYSIQUES VARIABLES

Résumé—Particulièrement pour les fluides à un seul composant, la variation des propriétés thermophysiques est négligeable sauf si les différences de température sont grandes et par suite elle n'a pas d'effet appréciable sur le transfert thermique. Par contre les propriétés thermophysiques peuvent varier significativement à cause des différences de concentration ce qui affecte le transfert de chaleur et de masse. On examine les effets de la variation de propriétés sur le transfert de chaleur et de masse par convection naturelle dans une cavité avec forces de flottement thermique et solutal. Les résultats indiquent que les variations des propriétés peuvent influencer nettement les transferts et la distribution de vitesse.

NATÜRLICHE KONVEKTION AUFGRUND HORIZONTALER TEMPERATUR- UND KONZENTRATIONSUNTERSCHIEDE—1. EINFLUSS VERÄNDERLICHER THERMOPHYSIKALISCHER STOFFEIGENSCHAFTEN

Zusammenfassung—Bei fluiden reinen Stoffen ist die Änderung der thermophysikalischen Eigenschaften meist vernachlässigbar und hat keinen nennenswerten Einfluß auf den Wärmetransport, wenn keine großen Temperaturunterschiede auftreten. Im Gegensatz dazu können sich Stoffeigenschaften aufgrund von Konzentrationsunterschieden erheblich ändern, was den Wärme- und Stofftransport beeinflußt. In der vorliegenden Arbeit wird der Einfluß der veränderlichen thermophysikalischen Stoffeigenschaften auf den Wärme- und Stofftransport in einem Hohlraum untersucht, indem natürliche Konvektion aufgrund thermisch- und konzentrationsbedingter Auftriebskräfte stattfindet. Die Ergebnisse zeigen, daß die Änderung der thermophysikalischen Stoffeigenschaften den Wärme- und Stofftransport und die Geschwindigkeitsverteilung erheblich beeinflussen können.

ЕСТЕСТВЕННАЯ КОНВЕКЦИЯ, ВЫЗВАННАЯ ГОРИЗОНТАЛЬНЫМИ ГРАДИЕНТАМИ ТЕМПЕРАТУРЫ И КОНЦЕНТРАЦИИ—1. ЭФФЕКТЫ ПЕРЕМЕННЫХ ТЕПЛОФИЗИЧЕСКИХ СВОЙСТВ

Аннотация—Для однокомпонентных жидкостей характерно пренебрежимо малое изменение теплофизических свойств (за исключением случаев больших разностей температур) и, следовательно, оно не оказывает существенного влияния на теплоперенос. Для жидких смесей теплофизические свойства могут значительно изменяться благодаря разности концентраций, влияющей на тепло- и массоперенос. В данной работе исследуется влияние изменения теплофизических свойств на тепло- и массоперенос в полости, обусловленный естественной конвекцией за счет совместного действия тепловых и массовых подъемных сил. Полученные результаты свидетельствуют о том, что изменения теплофизических свойств могут оказывать существенное влияние на тепло- и массоперенос и распределение скоростей.